

STRUCTURE AND ULTRASTRUCTURE STUDY ON THE POTENTIAL IMPACT OF GOLD NANOPARTICLES ON THE PERIODONTAL LIGAMENT OF ALBINO RATS

Mai El Sayed Shaaban Fakhr¹, Mervat Mohamed Youssef², Laila Sadek Ghali³

DOI: 10.21608/dsu.2022.97306.1082

Manuscript ID: DSU-2109-1082

KEYWORDS

Recovery, Toxicity,
PDL, AUNPs

ABSTRACT

Introduction: With the fast development of nanotechnology and its wide application within the biomedical field, the toxic effect of nanomaterials has attracted numerous attention. Consequently, a crucial subfield termed nan-toxicology has emerged, which is mostly defined because the study of the interactions between nanomaterials and biological systems with a stress on identifying the link between the physicochemical parameters and therefore the occurrence of toxic effects. **Aim:** The aim was to study the possible toxic effect of intraperitoneal administration of gold nanoparticles on the periodontal ligament of albino rats and moreover the possibility of one-month recovery period through hematoxylin and eosin stained sections for histological evaluation and transmission electron microscope for ultrastructural evaluation. **Material and Methods:** Forty-six male albino rats were employed in this investigation. They were divided into the subsequent groups: **Group (1)** (16 rats) served as controls, they received daily intraperitoneal injection of the solvent (deionized water 0.5 ml) for 21 days. **Group (2)** (15 rats) received 10mg/kg weight of AuNP solution intraperitoneally daily for 21 days. **Group (3)** (15 rats) were treated the identical way as Group 2 for 21 days and so left for one-month as a recovery period. The experiment lasted for 21 days for group 2 then the rats were euthanized by cervical dislocation. While the rats of group 3 were euthanized by cervical dislocation after 1 month of treatment stoppage with gold nanoparticles for recovery period; their lower jaws of each rat were dissected out, separated into two halves, the right halves were used for structural examination while the left halves were used for ultrastructural examination. **Results:** Examination of the PDL obtained from the group II animals showed marked dissociation and degeneration of collagen fiber bundles. The examined fibers of the rats which were allowed a recovery period showed improvement within the condition of structure and ultrastructural features of the fibers and cells of PDL. **Conclusion:** Our data suggest that AuNPs exert detrimental effects on cell structure and ultrastructure consequently cell function that would reverse following AuNPs removal.

INTRODUCTION

Nanotechnology is a prominent field that develops nanoparticles (NPs) and nanostructured products have many technological applications, like power generation, production of electronic devices, food industry, agriculture, and medicine. During this last area, many alternative sorts of nanomaterials are utilized in the last decades, like quantum dots, different metals, oxides, carbon-based nanoparticles, lipids, liposomes, and polymers of these materials present promising applications in image, diagnosis, and treatment ⁽¹⁾.

• E-mail address:
maisfakhr@gmail.com.

1. Assistant Lecturer, Oral Biology Department, Faculty of Dentistry, Sinai University.
2. Associate Professor, Head of Oral Biology Department, Faculty of Dentistry, Suez Canal University.
3. Professor of Oral Biology, Faculty of Dentistry, Cairo University.

Promising applications of gold nanoparticles (AuNPs) in nanomedicine include plasmon-based labeling and imaging, optical and electrochemical sensing, and diagnostics, which facilitate early detection and treatment of cancers⁽²⁾, hepatitis⁽³⁾, and tuberculosis⁽⁴⁾. Gold nanoparticles may be employed in angiogenesis, as antibacterial agents, in photothermal and radiofrequency-mediated thermal therapies⁽⁵⁾, in addition as delivery vehicles for genetic materials⁽⁶⁾, imaging agents⁽²⁾, and medicines⁽⁷⁾. AuNP's are widely preferred in nanotechnology based medicine because of their conjugation ability with several bio-molecules, such as proteins, enzymes, amino acids and DNA, and holding of high optical extinction coefficients⁽⁸⁾.

These applications have supported the soundness and unique properties of AuNPs similarly because of the ability to simply translocate target cells, thereby enhancing sustained release of medicine and increasing therapeutic efficacy⁽⁹⁾. there's however an excellent concern since during synthesis and development for a large range of applications, AuNPs of various sizes, shapes, and surface charges are generated and will be of health risk.

The toxicological behavior of gold nanoparticles are often influenced by the physicochemical properties, including size, shape, surface charge, and other factors, like methods utilized within the synthesis of gold nanoparticles, models used, dose, in vivo route of administration, and interference of gold nanoparticles within vitro toxicity assay systems⁽¹⁰⁾.

The requirement to know nanoparticles in a very biological environment is now shared by nanobiology, nanomedicine and nanotoxicology. Thus, nanotoxicity is an emerging field of research, a response to growing uses of nanosized materials during a slew of technological, medical applications and consumer products.

This investigation was designed to study the possible toxic effect of intraperitoneal administration of gold nanoparticles on the periodontal ligament of albino rats and possibility of one-month recovery period through:

- Hematoxylin and eosin stained sections for histological evaluation.
- Ultrastructural evaluation through transmission microscopy examination.

MATERIAL AND METHODS

The present research was waived from the approval of the Research Ethics Committee (REC) (138/2018) of the Faculty of Dentistry, Suez Canal University.

Forty-six adult male albino rats with an average 150-180gram body weight were used in the present investigation.

Animals were divided randomly into three groups as follows:

- **Group 1:** consisted of 16 rats that divided into 2 sub groups: they received daily intraperitoneal injection of the solvent, served as controls and divided equally into:

Sub group 1.1: consisted of 8 rats, received daily intraperitoneal injection of the solvent (deionized water 0.5 ml) for 21 days,

Sub group 1.2: consisted of 8 rats that received the same treatment as sub group 1.1 then left untreated for 1 month as a self recovery period.

- **Group 2:** consisted of 15 rats, they received daily intraperitoneal injection of 10mg/kg b.w of AuNP solution⁽¹¹⁾ dissolved in 0.5ml deionized water (particle sizes around 30 nm)⁽¹²⁾ for 21 days.

- **Group 3:** consisted of 15 rats, they were treated the same way as group 2 for 21 days and then left untreated for 1 month as a recovery period.

Preparation and characterization of the gold nanoparticles:

The rapid green method⁽¹³⁾ was used; it had been wiped out the Nanotechnology Lab, Faculty of Science, South Valley University.

Pomegranate fruits were collected from the local market. Chloroauric acid (International Company for Scientific and Medical Supply, Alfa Aesar, Germany) (> 99.9%), All glass-wares and pomegranate fruit were properly washed with de-ionized water and dried in the oven. Fruit peel extract (FPE) of pomegranate was used as a reductant which reduces the scale of gold particles to nanosize.

Properly washed 50g of fresh peels of the fruit were added in 250ml ultra-pure water in 500ml Erlenmeyer flask and boiled for 10-15mins. What man paper (No. 40) was used for filtration of boiled material to organize an aqueous fruit peel extract, which was used as such for metal nanoparticle synthesis.

An aqueous solution (1mM) of chloroauric acid solution was prepared and 50 ml of the metal (Au) ion solution was reduced using 1.8ml of FPE at temperature for 5mins. Below this FPE quantity, the answer takes quite 10mins to urge a big SPR for the metal nanoparticle. As a result pink-red colour solution, indicating the formation of gold nanoparticles was achieved after the addition of FPE.

Spectral analysis for the event of nanoparticles at different reaction conditions was observed by UV-Vis spectroscopy employing a Perkin-Elmer Lamda-45 spectrophotometer.

The progress of the reaction between metal ions and also the leaf extracts were monitored by UV-visible spectra of Au nanoparticles in solution with

different reaction times. The height within the spectrum of AuNPs was observed ~550nm.

Transmission electron microscope (TEM) JEM-1200EX, JEOL 1010 was used for the scale and shape analysis of developed nanoparticles. For TEM measurements, 3 μ l of the sample solution was placed on copper grid making a skinny film and kept for drying at temperature for 15mins, then extra sample was removed using the cone of a paper and reserved in grid box.

The experiment lasted for 21 days for group 2 then the rats were euthanized by cervical dislocation. While the rats of group 3 were euthanized by cervical dislocation after 1 month of treatment stoppage with nanogold for recovery; their lower jaws of every rat were dissected out, separated into two halves, the correct halves were fixed in 10% neutral buffered formalin, decalcified in 10% EDTA solution.

After complete decalcification, the specimens of the molar region were processed and embedded in paraffin. Four microns thick sections were cut to be stained with:

Hematoxylin and eosin stain for histological examination and detection of any structural changes in the periodontal ligament.

Preparation for Transmission Electron Microscope

Jaw specimens of the left side (using a modified Karnovsky 1965 solution)⁽¹⁴⁾ were immediately fixed in 2.5% buffered glutaraldehyde + 2% paraformaldehyde in 0.1M sodium phosphate buffer pH 7.4, left overnight at 4°C, washed 3 x 15 minutes (min.) in 0.1 M sodium phosphate buffer + 0.1 M Sucrose, postfixed 90 minutes in 2% sodium phosphate buffered osmium tetroxide pH 7.4, then the specimens' were decalcified in 10% EDTA. Ultra-thin sections (0.06 microns) were cut using ultra microtome and glass knives and then mounted on copper grids. Staining was carried out with

saturated uranyl acetate in 50% ethanol for 30 minutes, then washed for several times in distilled water followed by staining with lead citrate for 5 minutes to study the periodontal ligament by transmission electron microscope.

RESULTS

I. Histological Results: (Hematoxylin and Eosin stain)

The histological examination of hematoxylin and eosin stained sections of the correct halves of the lower jaws of the control group showed the conventional histological features of periodontal ligament which occupies the periodontal space between the cementum covering the basis of the tooth and also the bone forming the socket wall. The same as all other connective tissues, the PDL consists of cells, an extracellular compartment of collagenous fibers, a noncollagenous extracellular matrix, blood vessels, lymph vessels and nerves. The extracellular compartment consists of well-defined collagen fiber bundles embedded in an amorphous background material, referred to as ground substance. The collagen fibers are arranged in three principal groups, gingival group, transeptal group and alveolo-dental group of fibers (Fig. 1A & 1B).

In between the collagen fibers, interstitial spaces are found that contain areolar connective tissues (Fig. 1B). Beside that the fibroblasts, which are the foremost predominant cell in PDL are arranged along the fibers having large basophilic nucleus that sometimes appeared elongated and having the direction of adjacent collagen fibers.

The control group animals showed normal appearance of the alveolar bone. Because it was formed of alveolar bone proper and supporting alveolar bone. The alveolar bone proper formed the inner walls of the sockets, containing the opening of

Zuckermandel and Hirschfeld canals (Fig. 1B & 1C).

The PDL obtained from the group II animals that received daily intraperitoneal injection of 10mg/kg b.w of AuNP solution for 21 days revealed degenerative changes within the variety of disorientation, detachments and dissociation of the fibers and infiltration of inflammatory cells. Frequent areas of loss of attachment of PDL fibers to the bone and/or cementum surfaces were seen. The fibroblasts seemed to be more or less rounded instead of being elongated (Fig. 2A & 2B).

Massive inflammatory cell infiltrate was observed within the PDL fibers related to focal areas of aggregated cells (Fig. 2A). Within the interradicular area multiple dilated vessels were seen (Fig. 2C).

The attachment epithelium of the animals of this group showed an excellent feature, which was their extreme apical migration (Fig. 2A).

Bone resorption was the foremost observed effect. Along the alveolar ridge borders, multinucleated osteoclasts were identified within their Howship's lacunae, making the borders eroded (Fig. 2C).

Widening of the bone marrow cavities was another finding observed during this group of animals (Fig. 2B).

The periodontal ligament of the animals of group III that were allowed a recovery period for one-month after 21 days of intraperitoneal treatment with gold nanoparticles showed marked improvement of their histological features compared to control group with slight condensation of the collagen fibers and fibroblasts of the PDL additionally to increased interstitial spaces filled with blood vessels (Fig. 3A & 3C).

Presence of the reversal lines also were decreased compared to group II, indicating turnover near the control (Fig. 3B).

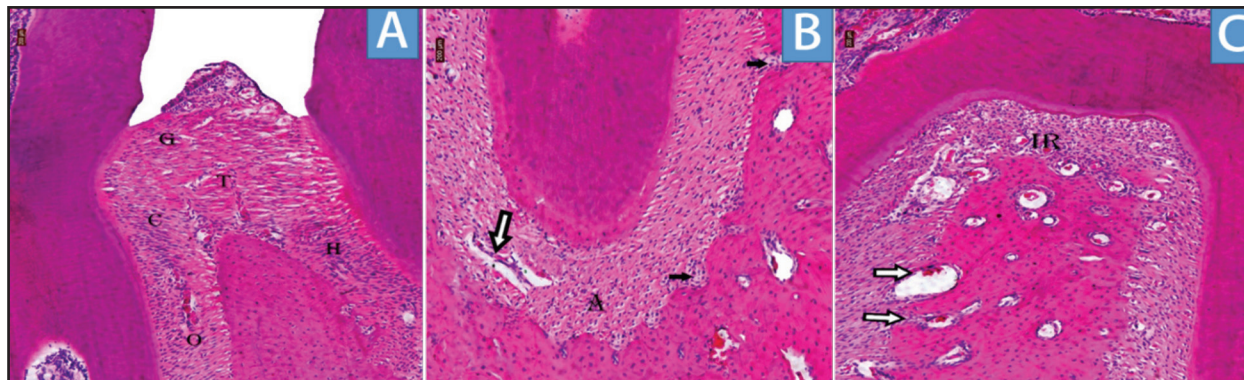


Fig. (1) A photomicrograph of PDL of control animal showing **A-** Higher magnification of the Gingival (G), Transeptal (T), Alveolar crest (C), Horizontal (H) and Oblique fibers (O). **B-** Higher magnification of the apical fibers, Zuckerkandle and Hirschfeld canals (black arrows) and interstitial space (white arrow). **C-** Interradicular fibers (IR) and alot of Zuckerkandle and Hirschfeld canals (arrows). (H&E, orig. mag. A-100 , B-100, C-100).

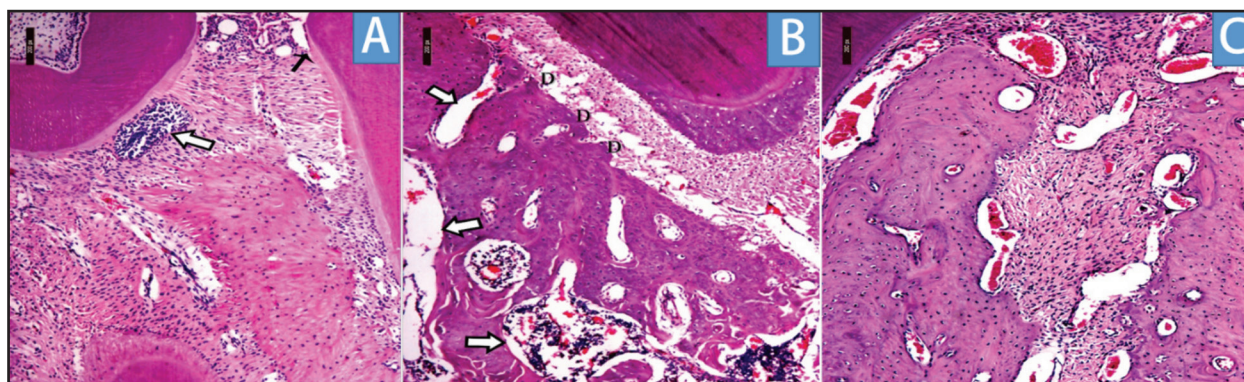


Fig. (2) A photomicrograph of PDL of group II animal showing **A-** Marked dissociation of the PDL fibers, massive inflammatory cells (white arrow) and apical migration of attachment epithelium (black arrow). **B-** Dissociated collagen fibers with focal areas of detachment from the alveolar bone (D) from cementum side with widened marrow cavities (arrows). **C-** Multiple dilated blood vessel in the interradicular area. (H&E, orig. mag. A-100 , B-100, C-100).

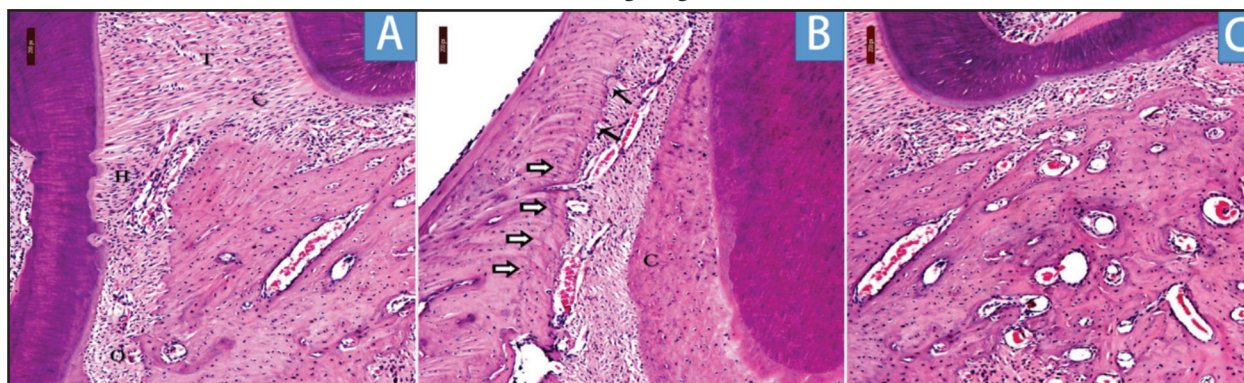


Fig. (3) A photomicrograph of PDL of group II animal showing **A-** Marked dissociation of the PDL fibers, massive inflammatory cells, and apical migration of attachment epithelium (black arrow). **B-** Dissociated collagen fibers with focal areas of detachment from the alveolar bone (D) from cementum side with widened marrow cavities (arrows). **C-** Multiple dilated blood vessel in the interradicular area. (H&E, orig. mag. A-100 , B-100, C-100).
 a photomicrograph of PDL of group III animal showing **A-** Normal appearance of Transeptal (T), Alveolar crest (C), Horizontal (H) and Oblique (O) PDL fibers. Notice plenty of interstitial spaces (arrows). **B-** Less reversal lines (white arrows) in the alveolar bone, empty Howships lacunae on the bone side (black arrows) and regeneration on the root side with cementoid formation (C). **C-** Improvement in the condition of the periodontal fibers in apical area with slight dilatation of blood vessels. (H&E, orig. mag. A-100 , B-100, C-100).

II. Electron microscopic results:

The microscopy examination of the PDL of control animals revealed normal ultrastructural features. The PDL was composed of collagen fibers that were cut longitudinally or transversely extending between bone and also the cementum, between cementum and cementum of adjacent teeth crossing above the interdental bone or extending from cementum to lamina propria of the gingiva (Fig. 4A & 4B).

Fibroblasts were the predominant cell within the PDL, per the direction of the section fibroblasts were either spindle, stellate or rounded in shape. The fibroblasts were presented with large rounded or oval nuclei with peripheral chromatin condensation. The nuclear membrane was smooth and regular, the cytoplasm showed abundant rough endoplasmic reticulum, vesicle, variable sized mitochondria, and occasional lysosomal bodies.

Neutrophils, mast cells, plasma cells, lymphocytes and macrophages were sometimes encountered within the animal tissue of the PDL (Fig. 4B).

The PDL obtained from the group II animals that received daily intraperitoneal injection of 10mg/kg

b.w of AuNP solution for 21 days showed marked dissociation and degeneration of collagen fiber bundles related to reduction in their density, fragmentation of fibers and loss of their orientation, leaving lots of debris that were frequently encountered (Fig. 5A & 5B). Fibroblasts showed signs of degeneration as they appeared shrunken with pyknotic nuclei, degenerated organelles, and fatty infiltration (Fig. 5B).

An apparent increase within the number of lymphocytes and plasma cells was observed with signs of degeneration (Fig. 5B). Marked dilatation of blood vessels with swollen endothelial cell lining, were observed (Fig. 5A).

The periodontal ligament of the group III animals that were allowed a recovery period for one-month after 21 days of intraperitoneal treatment with gold nanoparticles showed improvement within the condition of ultrastructural features of the fibers and cells of PDL (Fig. 6A & 6B). Collagen fibers appeared with almost normal orientation and density, where the collagen was arranged in bundles. Fibroblasts were found between the collagen bundles, a number of them showed the traditional ultrastructural appearance.

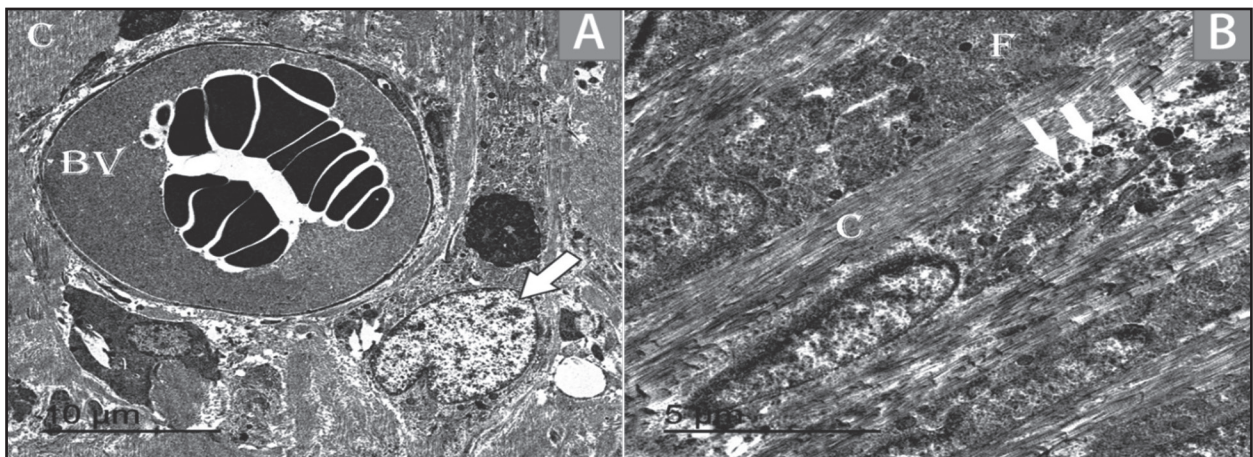


Fig. (4) An electron photomicrograph of PDL of a control animal showing **A**- Normal collagen fibers (C), macrophage cell (arrow) and blood vessels (BV). **B**- Normal collagen fibers (C) and fibroblast cells (F) having a lot of mitochondria (arrows). (Uranyl acetate & lead citrate. A- x 500, B- x 1200).

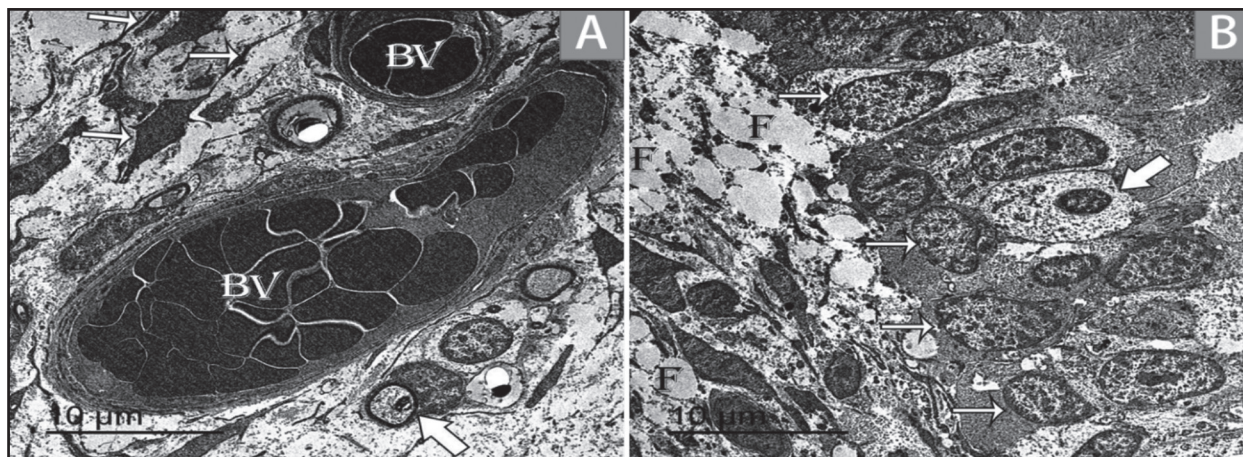


Fig. (5) An electron photomicrograph of PDL of group II animals showing A- Degenerated fibroblast cells (thin arrows) and markedly dilated blood vessels (BV) surrounded by degenerated collagen fibers. Notice myelinated nerve fibers (thick arrow). B- Multiple lymphocyte cells (thin arrows) and degenerated fibroblast cells with fatty infiltration (F) surrounded by degenerated collagen fibers. Notice the presence of plasma cell (thick arrow). (Uranyl acetate & lead citrate. A- x 500, B- x 500).

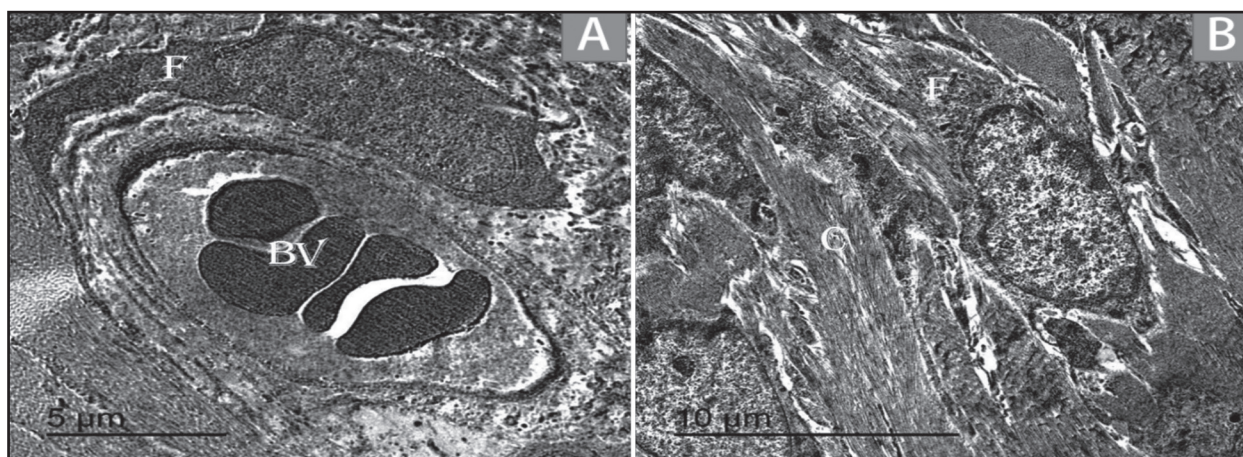


Fig. (6) An electron micrograph of PDL of group III animal showing A- Normal blood vessel (BV) and normal fibroblast cell (F). B- Normal fibroblast cells (F) and collagen fibers (C). (Uranyl acetate & lead citrate. A- x 1000, B- x 800).

DISCUSSION

Metallic nanoparticles, specifically AuNPs, offer a good spectrum of applications in biomedicine. A vital issue is their cytotoxicity, which depends greatly on various factors, including morphology of nanoparticles. Because metallic nanoparticles have a control on plasma membrane integrity, their shape and size may affect the viability of cells, thanks to

their different geometries similar to physical and chemical interactions with cell membranes. Variations within the size and shape of gold nanoparticles may indicate particular nanoparticle morphologies that provide strong cytotoxicity effects⁽¹⁵⁾.

Thus, the aim of this study was to review the potential impacts of gold nanoparticles on the periodontal ligament.

Rapid green method was employed in this study because it's cheap, easily available and eco-friendly reducing agents within the synthesis of AuNPs (16).

The authors are reported that Pomegranate extract is primarily composed of alkaloids and polyphenols. The active constituent that appears to be answerable for its multiple health benefits is Ellagic acid. Ellagic acid may be a present phenolic compound found in several fruits and nuts. Pomegranate extract has demonstrated a range of beneficial functions including antioxidant and anti-viral activity (17).

In in-vivo models, Chen *et al* (18), observed that the toxicity of AuNPs is also influenced by sex differences affecting males quite females, thus male albino rats were chosen as experimental models during this study.

In the current study rats received daily intraperitoneal injection of 10mg/kg b.w of AuNP solution dissolved in 0.5 ml deionized water (particle sizes around 30 nm) for 21 days. The intraperitoneal injection route was used over other intake routes because the literature showed preference of intraperitoneal injection in term of toxicity.

In agreement with our results, Tang *et al.* (19) stated that when the concentration of gold nanoparticles was increased to 10g/ml, the number of ROS induced within the A549 cells exceeded the conventional reactive oxygen species (ROS) generation required for cell survival, thus imposing toxic effects to the cells.

The particle sizes within the current study were also recommended by Pissuwan *et al.* (20) who reported that spherical AuNPs between 20–30 nm in diameter are capable of targeting cells through active and passive means, which is probably going to induce physiological changes following the cellular interaction between the AuNPs and target cells in vivo.

The ultra-small particles are characterized by their large surface areas which will lead to the direct formation of ROS that provides rise to cellular damage by damaging the DNA, proteins, and membranes and alter the foremost functions of mitochondria, cytoplasm and nucleus. (21) Therefore, oxidative stress could be a possible mechanism for the induced toxicity of GNPs on DNA and different organs. These alterations presented a transparent size-dependence, because the 30 nm AuNPs showed injurious effects, detected by their nuclear location and their higher DNA damage and this can be in accordance with our study (22).

The histological results of the current study revealed that collagen fibers of the periodontal ligament of rats treated with gold nanoparticles suffered dissociation and degeneration with apparent decrease within the number of fibroblasts additionally to massive inflammatory cell infiltrate was observed within the PDL fibers related to focal areas of aggregated cells and dilatation of the blood vessels was observed.

The degenerated collagen fibers seen within the tissues under investigation might be because of degenerative changes recorded within the fibroblasts causing failure or defective collagen synthesis. This could be not mention as excessive collagenase production by neutrophils.

Dilatation of the blood vessels was observed in our results, this was in agreement with Almansour and Jarrar (24) who reported that microscopic examination of lung tissue of rats exposed to 10 nm GNPs showed congestion with dilated inter-alveolar septal capillaries and leakage of blood cells were seen. The looks of extra-vasated erythrocytes within the alveolar sacs may indicate compression because of edema and/or thickening of the alveolar walls.

Bone resorption, in our study, was the most observed effect. Along the alveolar process borders,

multinucleated osteoclasts were identified within their lacunae, making the borders eroded. Widening of the bone marrow cavities was another finding observed in group II animals. These wide bone marrow cavities were associated with hyperemia.

These results were supported by Hallab *et al.* (25) who stated that within the presence of metal ions osteoblasts are able to release proinflammatory cytokines into the microenvironment, like transforming protein beta 1 (TGF- β 1), tumor necrosis factor alpha TNF- α , interleukin beta 1 (IL- β 1) and, most ordinarily, IL-6. These cytokines can successively, activate the differentiation of preosteoclasts into mature bone resorbing cells(26).

The microscopy examination of the periodontal ligament of gold nanoparticles group came to support the previously mentioned histological results. Where it showed marked dissociation and degeneration of collagen fiber bundles related to the reduction in their density, fragmentation of fibers and loss of their orientation, leaving lots of debris frequently encountered and shown foamy macrophage cells appeared with abnormal nuclear folding. Fibroblasts showed signs of degeneration as they appeared shrunken with pyknotic nuclei, degenerated organelles and cytoplasmic vacuolizations.

Our results agreed with those obtained by Taggart *et al.* (27) who reported that mitochondria is taken into account as an extra-nuclear target for AuNPs within the cell. Other studies supported the notion that the mode of necrobiosis induced by AuNPs is thru the intrinsic apoptotic pathway, in keeping with them ROS generated from the AuNPs activation and also the uncontrolled stress on endoplasmic reticulum can all disrupt the mitochondrial membrane potential and thus enhance the cytochrome-c release(28).

In agreement with our results, Almansour and Jarrar.(24) reported that diffuse and evenly diffused interstitial and peribronchial mononuclear inflam-

matory cell infiltration mainly lymphocytes was seen within the lungs of all members exposed to 10nm GNPs. Plasma cells and eosinophils were also seen.

The periodontal ligament of the animals of group III that were allowed a recovery period for one-month after 21 days of intraperitoneal treatment with gold nanoparticles showed marked improvement of their histological structures with slight condensation of the collagen fibers and fibroblasts of the PDL additionally to increased interstitial spaces filled with blood vessels. Osteoclastic activity gets decreased leaving empty Howship's lacunae.

With TEM, fibroblasts appeared almost normal and collagen fibers regained their orientation and arrangement in strong bundles. Alveolar bone showed normal appearance with osteoblast and bone lining cells representing new bone formation.

Mironava *et al.* (29) reported that the assembly of fibronectin partially recovers after five days and fully recovers after 14 days, whereas the assembly of collagen only slightly recovers after five days and remains not fully recovered after 14 days. So, the recovery period within the current study was one month to permit complete recovery.

Mironava *et al.* (29) also supported that following 14 days of recovery, the cytoskeleton of the cells exposed to both size particles completely recover and resemble that of the control cells. This is often coincided our investigation.

CONCLUSION

Most common toxicity modes related to nano-sized particles involve inflammation, degeneration, apoptosis and cellular damage. AuNPs' damage to cells and tissues isn't permanent but the recovery period of the experiment must be extended to permit complete recovery.

RECOMMENDATIONS

Further studies on tissue distribution, general behavioral changes, weight loss, mortality, inflammatory and oxidative stress responses, hematological analyses, tissue toxicological studies, and histopathological changes should be performed to justify the safe use of AuNPs in biomedical fields. These should be investigated to supply adequate information on both short- and long-term effects of AuNPs.

REFERENCES

1. Etheridge ML, Campbell SA, Erdman AG, Haynes CL, Wolf SM, McCullough J. The big picture on small medicine: the state of nanomedicine products approved for use or in clinical trials. *Nanomedicine nanotechnol, Biol Med.* 2013; 9-1.
2. Oh MH, Yu JH, Kim I, Nam YS. Genetically programmed clusters of gold nanoparticles for cancer cell-targeted photothermal therapy. *ACS Appl Mater Interfaces.* 2015; 7:22578-22586.
3. Shawky SM, Bald D, Azzazy HME. Direct detection of unamplified hepatitis C virus RNA using unmodified gold nanoparticles. *Clin Biochem.* 2010; 43:1163-1168.
4. Ng BYC, Xiao W, West NP, Wee EJH, Wang Y, Trau M. Rapid, single-cell electrochemical detection of Mycobacterium tuberculosis using colloidal gold nanoparticles. *Anal Chem.* 2015; 87:10613-10618.
5. Abadeer NS, Murphy CJ. Recent progress in cancer thermal therapy using gold nanoparticles. *J Phys Chem C.* 2016;120:4691-4716.
6. Pissuwan D, Niidome T, Cortie MB. The forthcoming applications of gold nanoparticles in drug and gene delivery systems. *J Control release.* 2011;149:65-71.
7. Brown SD, Nativo P, Smith J-A, et al. Gold nanoparticles for the improved anticancer drug delivery of the active component of oxaliplatin. *J Am Chem Soc.* 2010; 132:4678-4684.
8. Arvizo R, Bhattacharya R, Mukherjee P. Gold nanoparticles: opportunities and challenges in nanomedicine. *Expert Opin Drug Deliv.* 2010; 7:753-763.
9. Spivak MY, Bubnov R V, Yemets IM, Lazarenko LM, Tymoshok NO, Ulberg ZR. Gold nanoparticles-the theranostic challenge for PPPM: nanocardiology application. *EPMA J.* 2013; 4:18.
10. Thorat ND, Bauer J. Nanomedicine: next generation modality of breast cancer therapeutics. In *Nanomedicine for Breast Cancer Theranostics.* Elsevier. 2020:3-16.
11. Katsnelson BA, Privalova LI, Gurvich VB, et al. Comparative in vivo assessment of some adverse bioeffects of equidimensional gold and silver nanoparticles and the attenuation of nanosilver's effects with a complex of innocuous bioprotectors. *Int J Mol Sci.* 2013;14:2449-2483.
12. Lopez-Chaves C, Soto-Alvaredo J, Montes-Bayon M, Bettmer J, Llopis J, Sanchez-Gonzalez C. Gold nanoparticles: Distribution, bioaccumulation and toxicity. In vitro and in vivo studies. *Nanomedicine nanotechnol, Biol Med.* 2018;14:1-12.
13. Morris JK. A formaldehyde glutaraldehyde fixative of high osmolality for use in electron microscopy. *J cell Biol.* 1965; 27:1-149.
14. Ahmad N, Sharma S, Rai R. Rapid green synthesis of silver and gold nanoparticles using peels of Punica granatum. *Adv Mater Lett.* 2012;3:376-380.
15. Woźniak A, Malankowska A, Nowaczyk G, et al. Size and shape-dependent cytotoxicity profile of gold nanoparticles for biomedical applications. *J Mater Sci Mater Med.* 2017; 28:92.
16. Wu S, Yan S, Qi W, et al. Green synthesis of gold nanoparticles using aspartame and their catalytic activity for p-nitrophenol reduction. *Nanoscale Res Lett.* 2015; 10:213.
17. Ahmad N, Sharma S, Rai R. Rapid green synthesis of silver and gold nanoparticles using peels of Punica granatum. *Adv Mater Lett.* 2012; 3:376-380.
18. Chen J, Wang H, Long W, et al. Sex differences in the toxicity of polyethylene glycol-coated gold nanoparticles in mice. *Int J Nanomedicine.* 2013; 8:2409.
19. Tang Y, Shen Y, Huang L, et al. In vitro cytotoxicity of gold nanorods in A549 cells. *Environ Toxicol Pharmacol.* 2015; 39:871-878.
20. Pissuwan D, Cortie CH, Valenzuela SM, Cortie MB. Gold nanosphere-antibody conjugates for hyperthermal therapeutic applications. *Gold Bull.* 2007;40:121-129.

21. Lewinski N, Colvin V, Drezek R. Cytotoxicity of nanoparticles. *Small*. 2008; 4:26-49.
22. Lopez-Chaves C, Soto-Alvaredo J, Montes-Bayon M, Bettmer J, Llopis J, Sanchez-Gonzalez C. Gold nanoparticles: Distribution, bioaccumulation and toxicity. In vitro and in vivo studies. *Nanomedicine nanotechnol, Biol Med*. 2018; 14:1-12.
23. Forrester SJ, Kikuchi DS, Hernandez MS, Xu Q, Griendling KK. Reactive oxygen species in metabolic and inflammatory signaling. *Circ Res*. 2018; 122:877-902.
24. Almansour MI, Jarrar BM. Protective effect of propolis against pulmonary histological alterations induced by 10 nm naked gold nanoparticles. *Chiang Mai J Sci*. 2017; 44:414-426.
25. Hallab NJ, Vermes C, Messina C, Roebuck KA, Glant TT, Jacobs JJ. Concentration-and composition-dependent effects of metal ions on human MG-63 osteoblasts. *J Biomed Mater Res*. 2002; 60:420-433.
26. Kudo O, Sabokbar A, Pocock A, Itonaga I, Fujikawa Y, Athanasou NA. Interleukin-6 and interleukin-11 support human osteoclast formation by a RANKL-independent mechanism. *Bone*. 2003; 32:1-7.
27. Taggart LE, McMahon SJ, Currell FJ, Prise KM, Butterworth KT. The role of mitochondrial function in gold nanoparticle mediated radiosensitisation. *Cancer Nanotechnol*. 2014;5:1-12.
28. Huang Y-C, Yang Y-C, Yang K-C, et al. Pegylated gold nanoparticles induce apoptosis in human chronic myeloid leukemia cells. *Biomed Res Int*. 2014;2014.
29. Mironava T, Hadjiargyrou M, Simon M, Jurukovski V, Rafailovich MH. Gold nanoparticles cellular toxicity and recovery: effect of size, concentration and exposure time. *Nanotoxicol*. 2010;4:120-137.